



THE PAN-PACIFIC PLANET SEARCH. IV. TWO SUPER-JUPITERS IN A 3:5 RESONANCE ORBITING THE GIANT STAR HD 33844

ROBERT A. WITTENMYER^{1,2,3}, JOHN ASHER JOHNSON⁴, R. P. BUTLER⁵, JONATHAN HORNER^{2,3}, LIANG WANG⁶,
PAUL ROBERTSON^{7,8,13}, M. I. JONES⁹, J. S. JENKINS¹⁰, R. BRAHM¹¹, C. G. TINNEY^{1,2}, M. W. MENGEL³, AND J. CLARK¹²

¹School of Physics, University of New South Wales, Sydney 2052, Australia; rob@unsw.edu.au

²Australian Centre for Astrobiology, University of New South Wales, Sydney 2052, Australia

³Computational Engineering and Science Research Centre, University of Southern Queensland, Toowoomba, Queensland 4350, Australia

⁴Harvard-Smithsonian Center for Astrophysics, Cambridge, MA 02138, USA

⁵Department of Terrestrial Magnetism, Carnegie Institution of Washington, 5241 Broad Branch Road, NW, Washington, DC 20015-1305, USA

⁶Key Laboratory of Optical Astronomy, National Astronomical Observatories, Chinese Academy of Sciences,

A20 Datun Road, Chaoyang District, Beijing 100012, China

⁷Department of Astronomy and Astrophysics, The Pennsylvania State University, USA

⁸Center for Exoplanets & Habitable Worlds, The Pennsylvania State University, USA

⁹Department of Electrical Engineering and Center of Astro-Engineering UC, Pontificia Universidad Católica de Chile,

Av. Vicuña Mackenna 4860, 782-0436 Macul, Santiago, Chile

¹⁰Departamento de Astronomía, Universidad de Chile, Camino El Observatorio 1515, Las Condes, Santiago, Chile

¹¹Instituto de Astrofísica, Facultad de Física, Pontificia Universidad Católica de Chile and Millennium Institute of Astrophysics,

Av. Vicuña Mackenna 4860, 7820436 Macul, Santiago, Chile

¹²School of Physical Sciences, University of Adelaide, Adelaide SA 5005, Australia

Received 2015 October 8; accepted 2015 December 22; published 2016 February 4

ABSTRACT

We report the discovery of two giant planets orbiting the K giant HD 33844 based on radial velocity data from three independent campaigns. The planets move on nearly circular orbits with semimajor axes $a_b = 1.60 \pm 0.02$ AU and $a_c = 2.24 \pm 0.05$ AU, and have minimum masses ($m \sin i$) of $M_b = 1.96 \pm 0.12 M_{\text{Jup}}$ and $M_c = 1.76 \pm 0.18 M_{\text{Jup}}$. Detailed N -body dynamical simulations show that the two planets have remained on stable orbits for more than 10^6 years for low eccentricities and are most likely trapped in a mutual 3:5 mean motion resonance.

Key words: planetary systems – stars: individual (HD 33844) – techniques: radial velocities

1. INTRODUCTION

Surveys for planets orbiting evolved stars more massive than the Sun are well into their second decade. The longest-running surveys (e.g., Sato et al. 2005; Reffert et al. 2015) have been monitoring several hundred such stars for ~ 15 years. The combined efforts of these and other surveys have amassed enough data to begin making quantitative statements about the frequency and detailed properties of planetary systems beyond solar-type main-sequence stars.

An early prediction from formation models proposed that higher-mass stars should host higher-mass planets (Ida & Lin 2005), a prediction that is being borne out by observation (Bowler et al. 2010). Giant planet frequency has also been shown to increase with host star mass (Fischer & Valenti 2005; Bowler et al. 2010; Johnson et al. 2010), though with a drop-off for hosts with $M_* > 2.5 - 3.0 M_\odot$ (Omiya et al. 2009; Kunitomo et al. 2011; Reffert et al. 2015). Kretke et al. (2009) proposed a mechanism to explain the efficient formation of gas giant planets at orbital distances $a \gtrsim 1$ AU. For intermediate-mass stars, the inner edge of the magneto-rotational instability (MRI) dead zone lies far enough from the star to permit cores to accrete gas rapidly and produce gas giants at a higher rate than for solar-mass stars. An interesting consequence of their models is that the frequency of giant planets would have little dependence on stellar metallicity, in contrast to the well-known planet-metallicity correlation for dwarf stars (Fischer & Valenti 2005). However, recent results from Reffert et al. (2015) with a sufficiently large and self-consistent sample of

intermediate-mass stars and their planets in hand, show that planet occurrence remains positively correlated with metallicity for these stars.

The Pan-Pacific Planet Search (PPPS—Wittenmyer et al. 2011a) was a radial velocity survey of 170 southern giant stars using the 3.9 m Anglo-Australian Telescope (AAT) and its UCLES high-resolution spectrograph (Diego et al. 1990). It was originally conceived of as a southern hemisphere extension of the Lick and Keck Observatory survey for planets orbiting northern “retired A stars” (Johnson et al. 2006). The targets were selected to be redder ($1.0 < (B - V) < 1.2$) than the northern hemisphere sample to select for more metal-rich stars (Girardi et al. 2002). The PPPS operated from 2009 to 2014; papers detailing the spectroscopic stellar parameters and new planet detections are now in preparation (Wittenmyer et al. 2015b, 2016). This paper is organized as follows: Section 2 details the AAT and Keck observations of HD 33844 and gives the stellar parameters. Section 3 describes the orbit-fitting procedures and gives the parameters of the two planets in the HD 33844 system. In Section 4 we discuss the evidence for a planetary interpretation of the observed radial velocity variations, including dynamical stability simulations. We give our conclusions in Section 5.

2. OBSERVATIONS AND STELLAR PROPERTIES

HD 33844 is common to the AAT, Keck, and FEROS evolved-star surveys. Precision Doppler measurements for the PPPS are obtained with the UCLES echelle spectrograph at the AAT. The observing procedure is identical to that used by the long-running Anglo-Australian Planet Search (e.g., Butler et al.

¹³ NASA Sagan Fellow.

Table 1
AAT Radial Velocities for HD 33844

BJD-2400000	Velocity (m s ⁻¹)	Uncertainty (m s ⁻¹)
54867.00962	-14.89	1.63
55139.20744	-35.49	2.00
55525.14921	-2.27	1.97
55580.04370	-36.05	1.83
55601.94622	-51.59	1.79
55879.18697	4.37	2.28
55880.14794	3.28	1.75
55881.12234	-1.95	1.93
55906.00994	13.02	2.06
55968.97219	13.41	1.53
55993.93352	8.92	3.17
56051.85691	8.61	3.18
56343.96912	-1.05	2.30
56374.91336	3.36	1.82
56376.92296	3.92	1.79
56377.91375	0.00	1.44
56399.92598	16.56	2.37
56530.28448	8.68	2.28
56685.94081	-57.81	2.34
56747.87554	-64.48	2.16

2001; Tinney et al. 2001; Jones et al. 2010; Wittenmyer et al. 2012c); a 1 arcsec slit delivers a resolving power of $R \sim 45,000$. Calibration of the spectrograph point-spread function is achieved using an iodine absorption cell temperature-controlled at $60.0 \pm 0.1^\circ\text{C}$. The iodine cell superimposes a forest of narrow absorption lines from 5000 to 6200 Å, allowing simultaneous calibration of instrumental drifts as well as a precise wavelength reference (Valenti et al. 1995; Butler et al. 1996).

We have obtained 20 AAT observations of HD 33844 since 2009 February 4 and an iodine-free template spectrum was obtained on 2011 January 19. With $V = 7.29$, exposure times are typically 900–1200 s with a resulting S/N of ~ 100 –200 per pixel each epoch. The data given in Table 1 span a total of 1880 days (5.5 years) and have a mean internal velocity uncertainty of 2.1 m s^{-1} .

HD 33844 was also observed with the High Resolution Echelle Spectrometer (HIRES) on the 10 m Keck I telescope. A total of 36 epochs have been obtained spanning 2190 days (6 years). Radial velocities were computed using the iodine cell method as described above; the data are given in Table 2 and have a mean internal uncertainty of 1.3 m s^{-1} .

We also include 11 radial velocity observations from the FEROS spectrograph (Kaufer et al. 1999) on the 2.2 m telescope at La Silla Observatory. Those data are part of the EXPRESS (EXoPlanets aRound Evolved StarS) survey (Jones et al. 2011, 2015) for planets orbiting evolved stars. The PPPS and EXPRESS surveys have 37 targets in common; further papers are in preparation detailing joint planet discoveries made possible by the combination of the two data sets. The FEROS data for HD 33844 are given in Table 3; they cover a span of 1108 days and have a mean internal uncertainty of 3.9 m s^{-1} . The typical observing time was 250 s, leading to a S/N of 200 per pixel. The spectra were reduced using a flexible pipeline for echelle spectra (Jordan et al. 2014; R. Brahm et al. 2015, in preparation). The radial velocities were computed using the simultaneous calibration technique according to the method described in Jones et al. (2013) and Jones & Jenkins (2014).

Table 2
Keck Radial Velocities for HD 33844

BJD-2400000	Velocity (m s ⁻¹)	Uncertainty (m s ⁻¹)
54340.13214	29.1	1.2
54400.03609	20.0	1.2
54461.88282	3.4	1.4
54718.14825	-19.7	1.3
54791.07499	-10.8	1.4
54809.92924	-1.6	1.3
54839.01997	-0.4	1.4
54846.97020	-0.7	1.5
54864.91819	4.6	1.4
54929.72286	-11.5	1.5
55079.13055	-43.3	1.3
55109.10676	-31.3	1.3
55173.05357	-22.4	1.2
55187.90328	-13.5	1.3
55197.97134	-12.3	1.4
55229.77649	0.2	1.3
55255.74938	20.3	1.3
55285.78110	47.9	1.3
55312.72317	52.1	1.4
55428.13474	9.6	1.2
55456.04501	22.6	1.2
55490.96109	12.7	1.4
55521.97151	-3.1	1.4
55546.07504	-13.0	1.4
55584.91662	-35.2	1.3
55633.81481	-58.0	1.4
55791.13774	-33.8	1.2
55810.13994	-19.4	1.1
55902.01080	9.5	1.2
55904.86470	10.1	1.4
55931.98977	9.7	1.3
55960.77092	26.9	1.3
55972.77806	10.9	1.3
56197.06671	-18.9	1.3
56319.74545	7.3	1.4
56530.11001	14.2	1.3

Table 3
FEROS Radial Velocities for HD 33844

BJD-2400000	Velocity (m s ⁻¹)	Uncertainty (m s ⁻¹)
55457.83090	39.0	5.2
55612.57290	-55.3	3.8
56160.93800	-1.4	4.0
56230.78520	-10.3	3.9
56241.78170	-7.2	4.5
56251.83720	-23.6	2.6
56321.60110	15.8	3.7
56331.62140	24.1	3.9
56342.58360	23.9	3.5
56412.47550	8.8	4.6
56565.79190	-13.7	3.3

2.1. Stellar Properties

We have used our iodine-free template spectrum ($R \sim 60,000$, S/N ~ 200) to derive spectroscopic stellar parameters. In brief, the iron abundance [Fe/H] was determined from the equivalent widths of 32 unblended Fe lines and the LTE model atmospheres adopted in this work were interpolated from the ODFNEW grid of ATLAS9 (Castelli & Kurucz 2004). The effective temperature (T_{eff}) and bolometric correction (BC)

Table 4
Stellar Parameters for HD 33844

Parameter	Value	References
Spec. Type	K0 III	Houk & Smith-Moore (1988)
Distance (pc)	100.9 ± 6.5	van Leeuwen (2007)
($B - V$)	1.040 ± 0.009	Perryman et al. (1997)
$E(B - V)$	0.0290	...
A_V	0.0903	...
Mass (M_\odot)	1.78 ± 0.18	This work
	1.74 ± 0.18	Jones et al. (2011)
$V \sin i$ (km s ⁻¹)	<1	This work
	1.65	Jones et al. (2011)
[Fe/H]	+0.27 ± 0.09	This work
	+0.17 ± 0.10	Jones et al. (2011)
	+0.19 ± 0.12	Luck & Heiter (2007)
T_{eff} (K)	4861 ± 100	This work
	4890	Jones et al. (2011)
	4710	Massarotti et al. (2008)
	4886	Luck & Heiter (2007)
log g	3.24 ± 0.08	This work
	3.05	Jones et al. (2011)
	3.1	Massarotti et al. (2008)
v_t (km s ⁻¹)	1.00 ± 0.15	This work
	1.17	Jones et al. (2011)
	1.42	Luck & Heiter (2007)
Radius (R_\odot)	5.29 ± 0.41	This work
	5.33 ± 0.51	Jones et al. (2011)
Luminosity (L_\odot)	14.1 ± 1.8	This work
	14.4	Jones et al. (2011)
	12.6	Massarotti et al. (2008)
Age (Gyr)	1.88 ^{+0.76} _{-0.48}	This work

were derived from the color index $B - V$ and the estimated metallicity using the empirical calibration of Alonso et al. (1999, 2001). Since the color- T_{eff} method is not extinction-free, we corrected for reddening using $E(B - V) = 0.0290$ (Schlegel et al. 1998). The stellar mass and age were estimated from the interpolation of Yonsei-Yale (Y^2) stellar evolution tracks (Yi et al. 2003). The resulting stellar mass of $1.78 \pm 0.18 M_\odot$ was adopted for calculating the planet masses. Our derived stellar parameters are given in Table 4 and are in excellent agreement with the results of Jones et al. (2011) who found a mass of $1.74 \pm 0.18 M_\odot$ and a radius of $5.33 \pm 0.51 R_\odot$.

3. ORBIT FITTING AND PLANETARY PARAMETERS

Early AAT data for HD 33844 exhibited a periodicity of ~ 510 days, but the one-planet fit worsened with time until it could be tentatively fit with a second planet near ~ 900 days. Preliminary analysis of the AAT and Keck data together corroborated the two candidate periodicities. We first explored a wide range of parameter space by fitting the two data sets with a two-Keplerian model within a genetic algorithm (e.g., Horner et al. 2012; Wittenmyer et al. 2012a, 2013c). In brief, the genetic algorithm works on principles of evolutionary biology, producing an initially random population of planetary system parameters and then selecting the best-fit (lowest χ^2) models for “reproduction.” The next generation is then generated by perturbing the best-fit models (“mutation”) and repeating the process. The two planets were allowed to take on orbital periods in the range P_1 : 400–600 day and P_2 : 700–1200 day and eccentricities $e < 0.3$. A total of about 10^7 possible system configurations were tested in this manner. The best two-

planet solution was then used as a starting point for the generalized least-squares program *GaussFit* (Jefferys et al. 1988), which is used here to solve a Keplerian radial velocity orbit model as in our previous work (Tinney et al. 2011; Wittenmyer et al. 2011a, 2015c). As a further check, we performed a Keplerian fit optimized with a simplex algorithm using version 2.1730 of the *Systemic Console* (Meschiari et al. 2009) and estimated parameter uncertainties using the bootstrap routine therein on 100,000 synthetic data set realizations. We added 7 m s^{-1} of jitter in quadrature to the uncertainties of each of the three data sets. This jitter estimate is derived from 37 stable stars in the PPPS (334 measurements); their velocity distribution can be fit with a Gaussian of width $\sigma = 7 \text{ m s}^{-1}$. Since the planets are massive and move on orbits relatively close to each other (such that interactions can be expected), we also performed a dynamical fit using the Runge–Kutta integration method within *Systemic*. Table 5 gives the planetary system parameters resulting from both the Keplerian and dynamical fits; the results are indistinguishable and hence neither technique is clearly favored. The parameters given represent the mean of the posterior distribution and the 68.7% confidence interval. Using the host star mass of $1.78 M_\odot$ in Table 4, we derive planetary minimum masses of $1.96 \pm 0.12 M_{\text{Jup}}$ (HD 33844b) and $1.76 \pm 0.18 M_{\text{Jup}}$ (HD 33844c). The data and model fits for each planet are plotted in Figures 1–2.

4. DISCUSSION

4.1. Evidence for Orbiting Planets

Particularly for giant stars, where spots and pulsations can induce spurious radial velocity shifts with periods of hundreds of days, any claim of orbiting planets must be carefully examined to rule out intrinsic stellar signals (e.g., Hatzes & Cochran 2000; Reffert et al. 2015; Trifonov et al. 2015). For HD 33844, the periods of the two signals (551 and 916 days) are nowhere near the window function peaks at 384 and 8.1 days (AAT) or 30 and 364 days (Keck). Spurious periods in observational data commonly arise at those periods due to sampling (imposed by bright-time scheduling and the yearly observability of a given target).

To check whether the observed velocity variations could be due to intrinsic stellar processes, we examined the All-Sky Automated Survey (ASAS) V band photometric data for HD 33844 (Pojmanski & Maciejewski 2004). A total of 596 epochs were obtained from the ASAS All Star Catalog.¹⁴ We computed the mean magnitude per epoch over the five apertures then subjected the time series to an iterative sigma-clipping process. We removed points more than 3σ from the grand mean then recalculated the mean and its standard deviation. This process was performed three times, after which 511 epochs remained with a mean value of 7.28 ± 0.02 . The generalized Lomb–Scargle periodogram (Zechmeister & Kürster 2009) is shown in Figure 3 with the periods of the planets marked as dashed lines. While there are significant periodicities at 730 and 1250 days, there is little power near the periods of the candidate planets (551 and 916 days).

We also checked for correlation between the radial velocities and the equivalent width of the $H\alpha$ absorption line, which has been used as an activity indicator for giants (Hatzes et al. 2015)

¹⁴ <http://www.astrow.edu.pl/asas>

Table 5
HD 33844 Planetary System Parameters

Parameter	Keplerian Fit		Dynamical Fit	
	HD 33844b	HD 33844c	HD 33844b	HD 33844c
Period (days)	551.4 ± 7.8	916.0 ± 29.5	547.9 ± 6.4	924.3 ± 32.5
Eccentricity	0.15 ± 0.07	0.13 ± 0.10	0.16 ± 0.07	0.09 ± 0.08
ω (degrees)	211 ± 28	71 ± 67	190 ± 62	5 ± 30
K (m s^{-1})	33.5 ± 2.0	25.4 ± 2.9	32.9 ± 2.2	24.0 ± 2.2
T_0 (BJD-2400000)	54609 ± 41	54544 ± 164	54578 ± 50	54356 ± 281
$m \sin i$ (M_{Jup})	1.96 ± 0.12	1.75 ± 0.18	1.92 ± 0.11	1.68 ± 0.16
a (AU)	1.60 ± 0.02	2.24 ± 0.05	1.59 ± 0.01	2.25 ± 0.03
rms of fit—AAT (m s^{-1})	5.9		9.4	
rms of fit—Keck (m s^{-1})	7.2		7.2	
rms of fit—FEROS (m s^{-1})	10.7		11.6	
Total χ^2 (54 dof)	65.7		66.4	

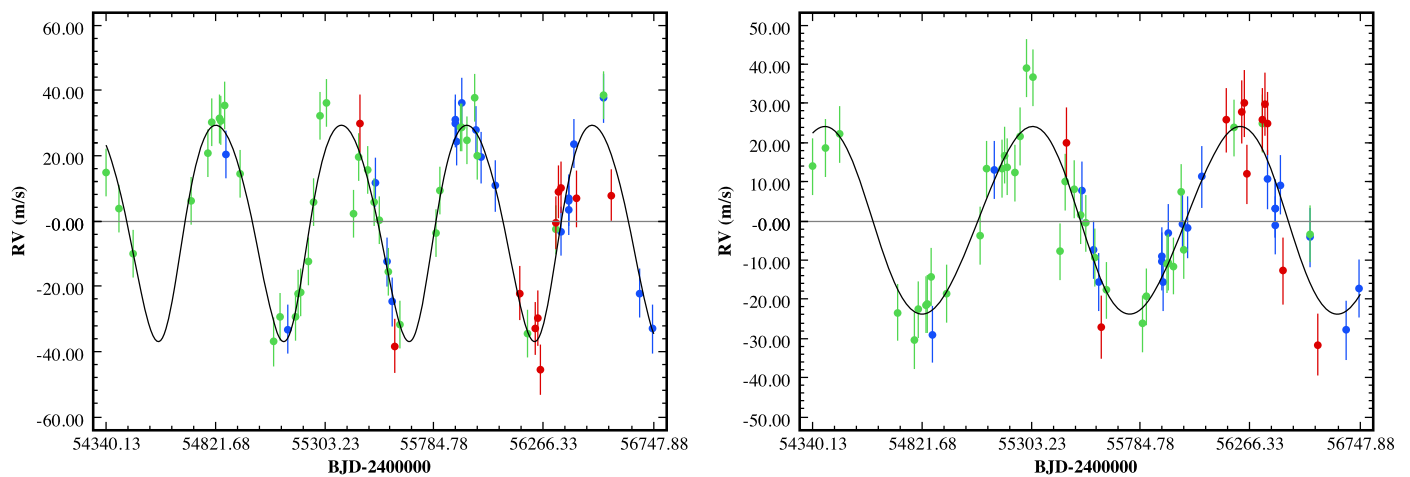


Figure 1. Left panel: data and Keplerian model fit for the inner planet HD 33844b, with the outer planet removed. Error bars are the quadrature sum of the internal uncertainties and 5 m s^{-1} of jitter. Right panel: same, but for the outer planet HD 33844c with the inner planet removed. The total rms about the two-planet Keplerian fit is 7.3 m s^{-1} . AAT—blue, Keck—green, FEROS—red.

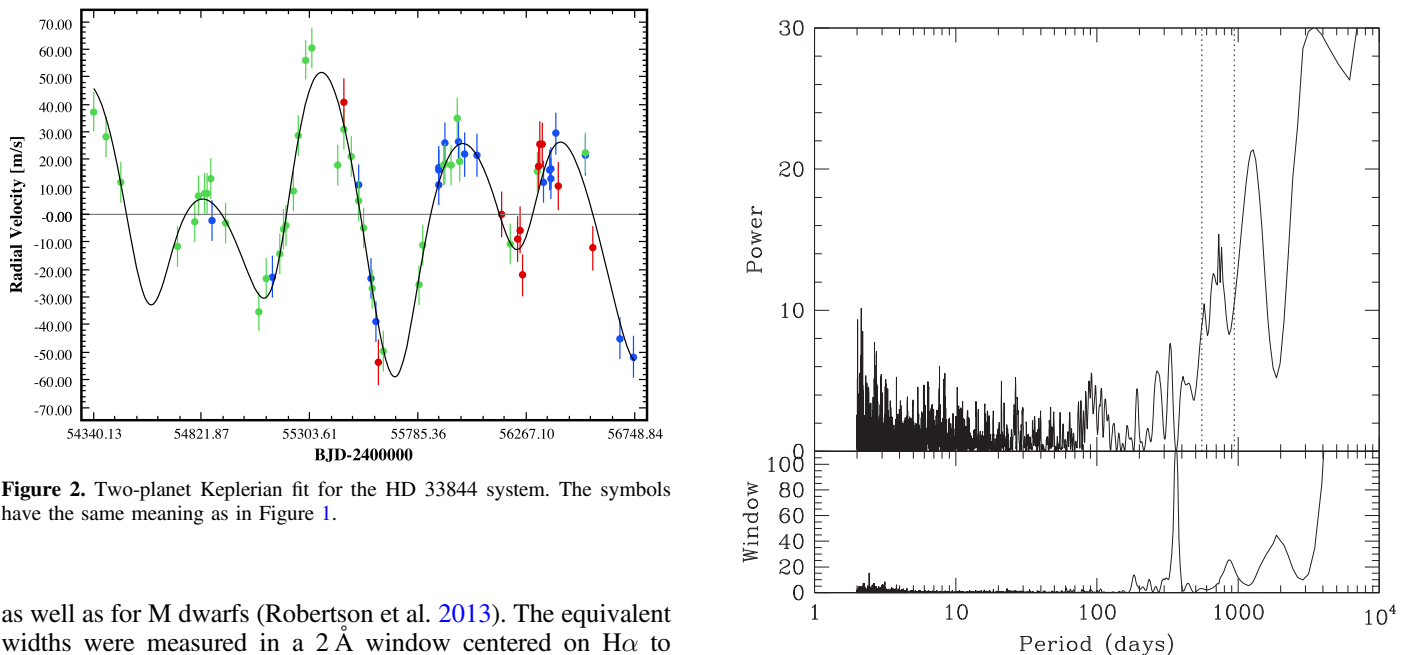


Figure 2. Two-planet Keplerian fit for the HD 33844 system. The symbols have the same meaning as in Figure 1.

as well as for M dwarfs (Robertson et al. 2013). The equivalent widths were measured in a 2 \AA window centered on $\text{H}\alpha$ to avoid contamination by telluric lines. A generalized Lomb–Scargle periodogram of the $\text{H}\alpha$ equivalent widths from the AAT spectra (Figure 4) shows no significant periodicities and

Figure 3. Generalized Lomb–Scargle periodogram of ASAS photometry for HD 33844. A total of 511 epochs spanning 8.8 years reveal no periodicities commensurate with the orbital periods of the planets (vertical dashed lines).

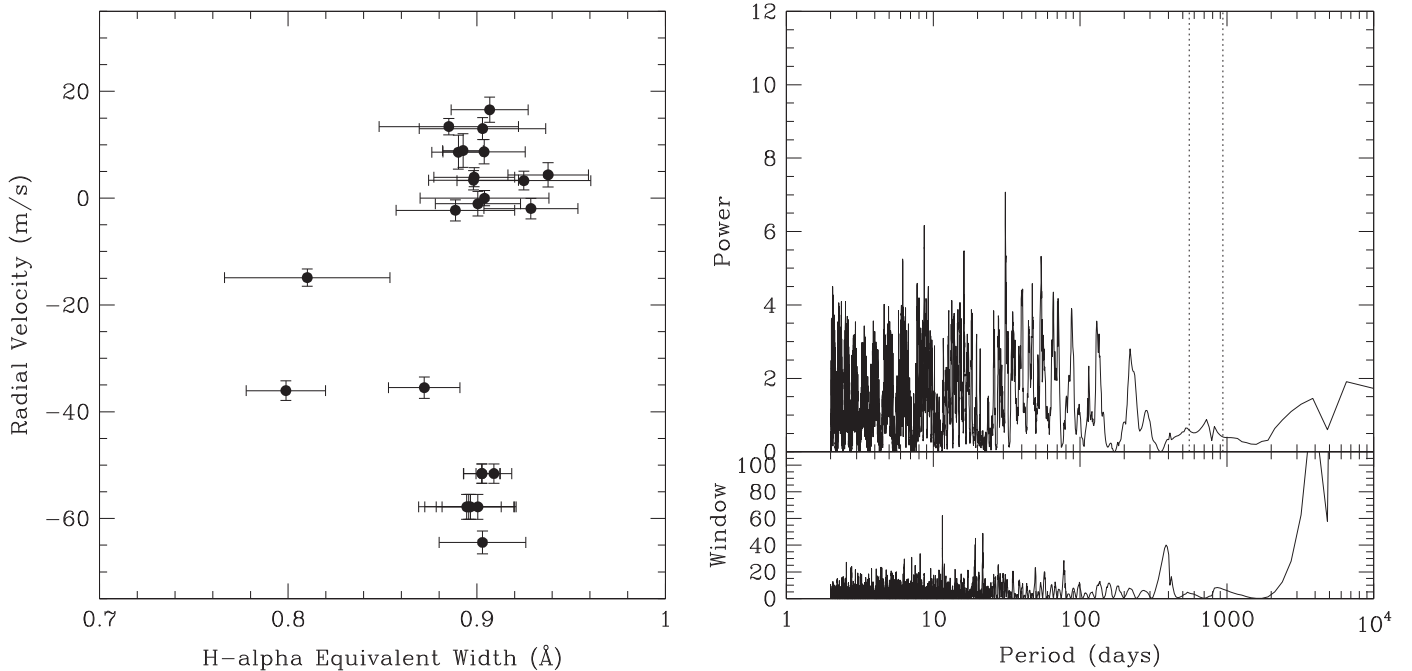


Figure 4. Left panel: AAT radial velocities and their H α equivalent widths. No correlations are evident. Right panel: generalized Lomb–Scargle periodogram of the H α measurements, again revealing no significant periodicities. The orbital periods of the planets are marked as vertical dashed lines.

there are no correlations with the velocities. Furthermore, the bisector velocity spans (defined as the velocity difference between line bisectors from the upper and lower part of an absorption line) computed from the FEROS spectra show no correlation with the radial velocities.

4.2. Dynamical Stability

The HD 33844 system appears to contain two super-Jupiter planets in orbits relatively close to each other. Given their mass and proximity, it is clearly important to consider whether the planets are dynamically feasible. That is, could planets on such tightly packed orbits be dynamically stable on timescales comparable to the lifetime of the system? A first estimate of the system’s stability can be garnered by simply assessing the dynamical separation of the two planets, considering the separation of their orbits compared to their mutual Hill radius. Following Gladman (1993), we can calculate the mutual Hill radius of the two planets as follows:

$$R_H = \left[\frac{(m_1 + m_2)}{3M_\odot} \right]^{1/3} \left[\frac{(a_1 + a_2)}{2} \right], \quad (1)$$

where the symbols have their usual meaning and the subscripts refer to the inner (1) and outer (2) planets respectively. Following this formulism, we find that the best-fit orbits for the two candidate planets are separated by 3.8 times their mutual Hill radius ($R_H = 0.167$ AU). For low-eccentricity orbits Gladman (1993) found that orbits became unstable at separations smaller than $\sim 2\sqrt{3} = 3.46 R_H$. The HD 33844 system is therefore close to this critical separation and as the proposed orbits are somewhat eccentric, it is clearly important to subject the proposed planets to further scrutiny. In contrast to widely separated systems such as HD 121056, (where the planets orbit at 0.4 and 3.0 AU—more than 9 mutual Hill radii apart), for which N -body simulations were not necessary, here

we must rigorously test the HD 33844 system stability as in our previous work (e.g., Marshall et al. 2010; Horner et al. 2013; Wittenmyer et al. 2013a).

Most interesting are those systems (e.g., Robertson et al. 2012a, 2012b; Wittenmyer et al. 2012b) for which the planets prove stable and dynamically feasible across just a small fraction of the potential orbital solutions. In these cases, which typically feature planets moving on or close to mutually resonant orbits, dynamical simulations serve a dual purpose. First, they provide evidence that supports the existence of the planets and secondly, they provide a strong additional constraint on the potential orbits followed by those planets, helping us to better tie down their true orbits than can be achieved on the basis of the observations alone.

Here, we study the stability of the candidate planets orbiting HD 33844 following a now well-established route. We created a suite of 126,075 copies of the HD 33844 system. In each of these cloned systems, the initial orbit of HD 33844b was the same, located at its nominal best-fit values (Table 5). For each system, we systematically varied the initial semimajor axis (a), eccentricity (e), argument of periastron (ω), and mean anomaly (M) of HD 33844c. The masses of the planets were held fixed at their minimum values ($m \sin i$, Table 5). We note that changing the mass of the planets could alter the stability of the system. This can be illustrated by examination of Equation (1): it is immediately apparent that if the masses of the planets are increased, so too is the size of their mutual Hill radius and thereby the strength of their mutual interaction. However, the effect is actually relatively small when compared with the influence of their orbital elements. As such, in this work we solely explore the influence of “element space” and leave the exploration of “mass space” for future work, once the orbital elements of the planets have been better constrained through followup observations. Once the uncertainties in those elements are sufficiently small, it might be possible to use “mass space” to constrain the maximum masses of the planets and thereby

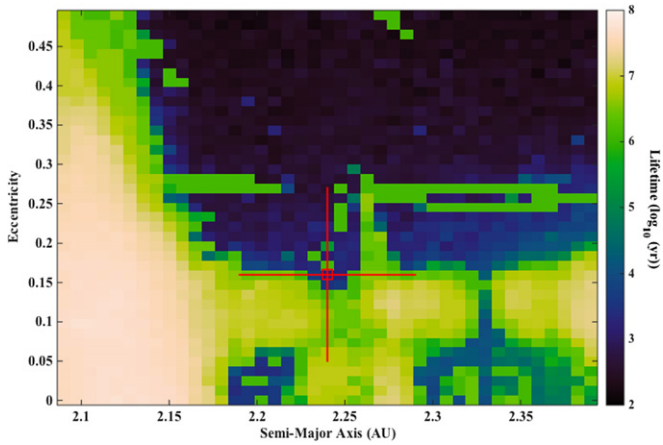


Figure 5. Dynamical stability for the HD 33844 system as a function of the initial semimajor axis and eccentricity of the outer planet. The best-fit orbit for that planet is marked by the open square and the crosshairs show the 1σ uncertainties. Configurations featuring eccentricities 1σ smaller than the nominal best fit generally remained stable for more than 10^6 years.

obtain some constraints on the inclination of the system to our line of sight, but such calculations are beyond the scope of this work. We do, however, note that a tentative upper limit on the masses of the planets can be obtained using the resonance overlap criterion (e.g., Wisdom 1980; Deck et al. 2013). This analytic estimate sets an upper bound of $\sim 10 M_{Jup}$ for each planet. As such, we can be fairly confident that the two bodies are planetary in nature rather than being brown dwarfs.

Since previous studies have shown that the stability of a system is most strongly dependent on semimajor axis and eccentricity, we tested 41 discrete values of each of these variables spanning the full $\pm 3\sigma$ uncertainty ranges. At each of the 1681 $a - e$ pairs created in this way, we tested 15 unique values of the argument of periastron and five of the mean anomaly, distributed in each case evenly across the 1σ uncertainty ranges in these variables. This gave us a total of 126,075 unique potential orbits for HD 33844c.

We then used the Hybrid integrator within the n -body dynamics package MERCURY (Chambers 1999) to follow the evolution of each of the test planetary systems for a period of 100 Myr. Simulations were stopped early if either of the planets were ejected from the system (upon reaching a barycentric distance of 5 AU, which would require significant strong instability between the two planets). They were also halted if either of the planets fell into the central star whose mass was set at $1.78 M_{\odot}$ or if they collided with one another. If any of these events happened, the time of collision/ejection was recorded and the simulation was brought to a close.

As a result of these simulations, we are able to examine the dynamical stability of the HD 33844 system as a function of the initial orbit on which HD 33844c was placed. Figure 5 shows the stability of the system as a function of the initial semimajor axis and eccentricity of that planet’s orbit. In Figure 6 we show how the orbital solutions tested in our dynamical simulations fit to the observed data, expressed in terms of the difference in total χ^2 relative to the best fit.

It is immediately clear from Figure 5 that the proposed orbital solution for the system lies in a region of complex dynamical behavior with both extremely stable and unstable solutions being possible. It is reassuring, however, to note that broad regions of dynamical stability lie comfortably within the

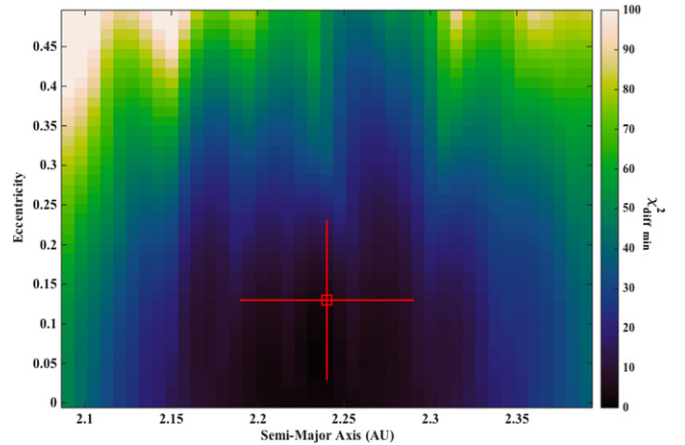


Figure 6. χ^2 difference compared with the best fit for the 126,075 system configurations tested in Figure 5 as a function of the initial semimajor axis and eccentricity of HD 33844c. At each $a - e$ location we show the minimum value of total χ^2 from the 75 ω -mean anomaly combinations tested therein (54 degrees of freedom).

1σ uncertainties on the proposed solution, particularly toward lower eccentricities. We note that least-squares radial velocity fitting routines are well-known to inflate eccentricities (e.g., Shen & Turner 2008; O’Toole et al. 2009; Wittenmyer et al. 2013c). That stability is due to orbits in that region being trapped in mutual 3:5 mean motion resonance with the orbit of HD 33844b. From Table 5 the Keplerian solution gives a period ratio of 1.661 and 1.687 for the dynamical fit. Within their uncertainties these solutions agree with each other and are wholly consistent with the 3:5 resonance (period ratio 1.667).

In addition to the central region of stability, orbits at smaller semimajor axes fall into a broad region of stability that extends across the full span of tested orbital eccentricities. This feature is the result of the mutual 2:3 mean motion resonance between HD 33844c and HD 33844b which is centered on 2.102 AU.

We can also see evidence of unstable resonant behavior through the plot. Most strikingly, there is a band of unstable solutions centered at 2.33 AU. This band is the result of the 4:7 mean motion resonance between the two planets. A further unstable resonant region can be seen around 2.195 AU, associated with the 5:8 resonance between the planets. Finally, the 5:9 resonance can be found at 2.375 AU, which is likely the cause of the sculpting of the stability of the system in that region.

As such, we can conclude that the candidate planets orbiting HD 33844 are dynamically feasible but that they most likely move on mutually resonant, low-eccentricity orbits. As a further check, we investigated the behavior of the resonant angles for a number of key resonances in the vicinity of the complicated “stability terrain” around the best-fit orbit. We found that the best-fit orbital solution is strongly influenced by its proximity to the 3:5 resonance. In particular, we found that the resonant angle $\phi = 5\lambda_2 - 3\lambda_1 - \omega_1 + \omega_2$ alternates between libration and circulation in a regular manner, completing three full cycles (one libration + one circulation) per 500 years of integration. A similar but noisier behavior was observed for a scenario in which the planets were located on orbits whose periods were in 5:8 commensurability. Here the resonant angle for the 5:8 mean motion resonance switched chaotically between periods of libration (lasting up to 1000 years) and period of smooth, slow circulation. The influence of

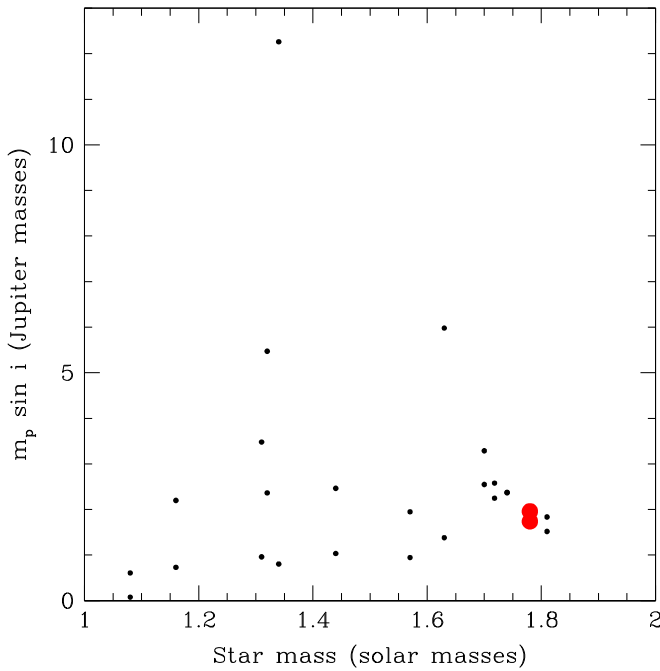


Figure 7. Minimum masses ($m \sin i$) of planets in multiple systems orbiting evolved stars ($\log g < 4.0$) as a function of stellar mass. Only 12 such systems are known; HD 33844 is shown as large red filled circles.

resonant interaction for these solutions was unmistakable, and given the proximity of the best-fit solution to the location of the 3:5 resonance, it seems most likely that the planets are trapped within it (although we note that the 5:8 and 7:12 mean motion resonances also fall within the 1σ uncertainty in semimajor axis) together with an abundance of higher-order weaker resonances.

5. CONCLUSIONS

We have given evidence for two super-Jovian mass planets orbiting the metal-rich ($[\text{Fe}/\text{H}] = +0.27 \pm 0.09$) giant, HD 33844. This result is consistent with findings from Reffert et al. (2015) and Maldonado et al. (2013) demonstrating that metal-rich stars with masses greater than $1.5 M_{\odot}$ are more likely to host planets. To date, relatively few systems of multiple giant planets are known to orbit evolved stars. Figure 7 shows the 12 previously known multiple-planet systems orbiting evolved stars ($\log g < 4.0$). The HD 33844 system is included as large red circles. HD 33844 is also a multiple-Jovian planet system in which all of the gas giants ($m \sin i > 0.2 M_{\text{Jup}}$) have low eccentricities ($e < 0.2$). Such a configuration is relatively uncommon (Harakawa et al. 2015), with only 15 systems known to date. Jones et al. (2015) noted that of the multiple-planet systems known to orbit evolved stars all but one of the host stars were first-ascent giants; HD 33844 adds to this count as it is near the base of the red giant branch. This is relevant because although the inner planet has a large orbital distance ($a \sim 1.6$ AU), it might eventually be engulfed in a distant future due to tidal interaction with the host star while the outer planet ($a \sim 2.3$ AU) might eventually survive such a process (e.g., Villaver & Livio 2007; Kunitomo et al. 2011; Mustill & Villaver 2012). As a result, in a distant future this system might evolve to a single-planet system, which is what we typically find around post-RGB stars as suggested by Jones et al. (2015).

It has been noted by Ghezzi et al. (2010) and Sousa et al. (2008) that there may be a correlation between the stellar metallicity and the masses of the planets, i.e., stars hosting only \sim Neptune-mass planets tend to have lower metallicity than stars hosting Jupiter-mass planets. In particular, Ghezzi et al. (2010) remarked that it is possible that “metallicity plays an important role in setting the mass of the most massive planet.” We have checked for the possibility of additional undetected planets using our well-established detection-limit methods (e.g., Wittenmyer et al. 2006, 2011b, 2013b). For our data on HD 33844, with a total residual rms of $7.3 m s^{-1}$ we can rule out the presence of additional planets with $m \sin i > 0.3 M_{\text{Jup}}$ interior to HD 33844b at 99% confidence. To push this limit down to the Neptune-mass regime, one must observe at higher cadence (Wittenmyer et al. 2015a) or adopt observing strategies specifically intended to mitigate stellar oscillation noise (O’Toole et al. 2008; Dumusque et al. 2011).

J.H. is supported by USQ’s Strategic Research Fund: the STARWINDS project. C.G.T. is supported by Australian Research Council grants DP0774000 and DP130102695. We gratefully acknowledge the efforts of PPPS guest observers Brad Carter, Hugh Jones, and Simon O’Toole. This research has made use of NASA’s Astrophysics Data System (ADS) and the SIMBAD database operated at CDS, Strasbourg, France. This research has also made use of the Exoplanet Orbit Database and the Exoplanet Data Explorer at exoplanets.org (Wright et al. 2011).

REFERENCES

- Alonso, A., Arribas, S., & Martínez-Roger, C. 1999, *A&AS*, **140**, 261
 Alonso, A., Arribas, S., & Martínez-Roger, C. 2001, *A&A*, **376**, 1039
 Bowler, B. P., Johnson, J. A., Marcy, G. W., et al. 2010, *ApJ*, **709**, 396
 Butler, R. P., Marcy, G. W., Williams, E., et al. 1996, *PASP*, **108**, 500
 Butler, R. P., Tinney, C. G., Marcy, G. W., et al. 2001, *ApJ*, **555**, 410
 Castelli, F., & Kurucz, R. L. 2004, in Proc. IAU Symp. 210, Modelling of Stellar Atmospheres, ed. N. Piskunov et al. (Dordrecht: Kluwer)
 Chambers, J. E. 1999, *MNRAS*, **304**, 793
 Deck, K. M., Payne, M., & Holman, M. J. 2013, *ApJ*, **774**, 129
 Diego, F., Charalambous, A., Fish, A. C., & Walker, D. D. 1990, Proc. SPIE, **1235**, 562
 Dumusque, X., Udry, S., Lovis, C., Santos, N. C., & Monteiro, M. J. P. F. G. 2011, *A&A*, **525**, A140
 Fischer, D. A., & Valenti, J. 2005, *ApJ*, **622**, 1102
 Ghezzi, L., Cunha, K., Smith, V. V., et al. 2010, *ApJ*, **720**, 1290
 Girardi, L., Bertelli, G., Bressan, A., et al. 2002, *A&A*, **391**, 195
 Gladman, B. 1993, *Icar*, **106**, 247
 Harakawa, H., Sato, B., Omiya, M., et al. 2015, *ApJ*, **806**, 5
 Hatzes, A. P., & Cochran, W. D. 2000, *AJ*, **120**, 979
 Hatzes, A. P., Cochran, W. D., Endl, M., et al. 2015, *A&A*, **580**, A31
 Horner, J., Wittenmyer, R. A., Hinse, T. C., et al. 2013, *MNRAS*, **435**, 2033
 Horner, J., Wittenmyer, R. A., Hinse, T. C., & Tinney, C. G. 2012, *MNRAS*, **425**, 749
 Houk, N., & Smith-Moore, M. 1988, in Michigan Catalogue of Two-dimensional Spectral Types for the HD Stars, Vol. 4, ed. N. Houk, & M. Smith-Moore (Ann Arbor, MI: Univ. Michigan) 14+505
 Ida, S., & Lin, D. N. C. 2005, *ApJ*, **626**, 1045
 Jefferys, W. H., Fitzpatrick, M. J., & McArthur, B. E. 1988, *CeMec*, **41**, 39
 Johnson, J. A., Aller, K. M., Howard, A. W., & Crepp, J. R. 2010, *PASP*, **122**, 905
 Johnson, J. A., Marcy, G. W., Fischer, D. A., et al. 2006, *ApJ*, **652**, 1724
 Jones, H. R. A., Butler, R. P., Tinney, C. G., et al. 2010, *MNRAS*, **403**, 1703
 Jones, M. I., & Jenkins, J. S. 2014, *A&A*, **562**, A129
 Jones, M. I., Jenkins, J. S., Rojo, P., & Melo, C. H. F. 2011, *A&A*, **536**, A71
 Jones, M. I., Jenkins, J. S., Rojo, P., Melo, C. H. F., & Bluhm, P. 2013, *A&A*, **556**, A78
 Jones, M. I., Jenkins, J. S., Rojo, P., Melo, C. H. F., & Bluhm, P. 2015, *A&A*, **573**, A3
 Jordan, A., Brahm, R., Bakos, G. A., et al. 2014, *AJ*, **148**, 29

- Kaufer, A., Stahl, O., Tubbesing, S., et al. 1999, *Msngr*, **95**, 8
- Kretke, K. A., Lin, D. N. C., Garaud, P., & Turner, N. J. 2009, *ApJ*, **690**, 407
- Kunitomo, M., Ikoma, M., Sato, B., Katsuta, Y., & Ida, S. 2011, *ApJ*, **737**, 66
- Luck, R. E., & Heiter, U. 2007, *AJ*, **133**, 2464
- Maldonado, J., Villaver, E., & Eiroa, C. 2013, *A&A*, **554**, A84
- Marshall, J., Horner, J., & Carter, A. 2010, *IJAsB*, **9**, 259
- Massarotti, A., Latham, D. W., Stefanik, R. P., & Fogel, J. 2008, *AJ*, **135**, 209
- Meschiari, S., Wolf, A. S., Rivera, E., et al. 2009, *PASP*, **121**, 1016
- Mustill, A. J., & Villaver, E. 2012, *ApJ*, **761**, 121
- Omiya, M., Izumiura, H., Han, I., et al. 2009, *PASJ*, **61**, 825
- O'Toole, S. J., Tinney, C. G., & Jones, H. R. A. 2008, *MNRAS*, **386**, 516
- O'Toole, S. J., Tinney, C. G., Jones, H. R. A., et al. 2009, *MNRAS*, **392**, 641
- Perryman, M. A. C., Lindegren, L., Kovalevsky, J., et al. 1997, *A&A*, **323**, L49
- Pojmanski, G., & Maciejewski, G. 2004, *AcA*, **54**, 153
- Reffert, S., Bergmann, C., Quirrenbach, A., Trifonov, T., & Künstler, A. 2015, *A&A*, **574**, A116
- Robertson, P., Endl, M., Cochran, W. D., et al. 2012a, *ApJ*, **749**, 39
- Robertson, P., Endl, M., Cochran, W. D., & Dodson-Robinson, S. E. 2013, *ApJ*, **764**, 3
- Robertson, P., Horner, J., Wittenmyer, R. A., et al. 2012b, *ApJ*, **754**, 50
- Sato, B., Kambe, E., Takeda, Y., et al. 2005, *PASJ*, **57**, 97
- Schlegel, D. J., Finkbeiner, D. P., & Davis, M. 1998, *ApJ*, **500**, 525
- Shen, Y., & Turner, E. L. 2008, *ApJ*, **685**, 553
- Sousa, S. G., Santos, N. C., Mayor, M., et al. 2008, *A&A*, **487**, 373
- Tinney, C. G., Butler, R. P., Marcy, G. W., et al. 2001, *ApJ*, **551**, 507
- Tinney, C. G., Wittenmyer, R. A., Butler, R. P., et al. 2011, *ApJ*, **732**, 31
- Trifonov, T., Reffert, S., Zechmeister, M., et al. 2015, *A&A*, **582**, A54
- Valenti, J. A., Butler, R. P., & Marcy, G. W. 1995, *PASP*, **107**, 966
- van Leeuwen, F. 2007, *A&A*, **474**, 653
- Villaver, E., & Livio, M. 2007, *ApJ*, **661**, 1192
- Wisdom, J. 1980, *AJ*, **85**, 1122
- Wittenmyer, R. A., Butler, R. P., Wang, L., et al. 2016, *MNRAS*, **455**, 1398
- Wittenmyer, R. A., Endl, M., Cochran, W. D., et al. 2006, *AJ*, **132**, 177
- Wittenmyer, R. A., Endl, M., Wang, L., et al. 2011a, *ApJ*, **743**, 184
- Wittenmyer, R. A., Gao, D., Hu, S. M., et al. 2015a, *PASP*, **127**, 1021
- Wittenmyer, R. A., Horner, J., & Marshall, J. P. 2013a, *MNRAS*, **431**, 2150
- Wittenmyer, R. A., Horner, J., Marshall, J. P., Butters, O. W., & Tinney, C. G. 2012a, *MNRAS*, **419**, 3258
- Wittenmyer, R. A., Horner, J., & Tinney, C. G. 2012b, *ApJ*, **761**, 165
- Wittenmyer, R. A., Horner, J., Tuomi, M., et al. 2012c, *ApJ*, **753**, 169
- Wittenmyer, R. A., Liu, F., Wang, L., et al. 2015b, *AJ*, submitted
- Wittenmyer, R. A., Tinney, C. G., Horner, J., et al. 2013b, *PASP*, **125**, 351
- Wittenmyer, R. A., Tinney, C. G., O'Toole, S. J., et al. 2011b, *ApJ*, **727**, 102
- Wittenmyer, R. A., Wang, L., Liu, F., et al. 2015c, *ApJ*, **800**, 74
- Wittenmyer, R. A., Wang, S., Horner, J., et al. 2013c, *ApJS*, **208**, 2
- Wright, J. T., Fakhouri, O., Marcy, G. W., et al. 2011, *PASP*, **123**, 412
- Yi, S. K., Kim, Y.-C., & Demarque, P. 2003, *ApJS*, **144**, 259
- Zechmeister, M., & Kürster, M. 2009, *A&A*, **496**, 577